THE ASTROPHYSICAL JOURNAL, 418:L41–L44, 1993 November 20

THE EXTREME ULTRAVIOLET SPECTRUM OF ALPHA AURIGAE (CAPELLA)

A. K. DUPREE,[1,2] N. S. BRICKHOUSE,[2] G. A. DOSCHEK,[1,3] J. C. GREEN,[1,4] AND J. C. RAYMOND[1,2]

Received 1993 August 5; accepted 1993 September 7

ABSTRACT

Extreme ultraviolet spectra ($\lambda\lambda$ 70–740) of the bright spectroscopic binary system, Capella (Alpha Aurigae) obtained with the *Extreme Ultraviolet Explorer* satellite (*EUVE*), show a rich emission spectrum dominated by iron emission lines: Fe XV–XXIV. The emission measure for the system reveals a continuous distribution of plasma temperatures between 10^5 and $10^{7.8}$ K, with a clear minimum near 10^6 K and a local maximum at 6×10^6 K. Electron density diagnostics based on Fe XXI indicate $N_e \approx 4 \times 10^{11}$–$10^{13}$ cm^{-3} at $T_e = 10^7$ K.

Subject headings: stars: chromospheres — stars: giant — stars: mass loss — stars: individual (α Aurigae)

1. INTRODUCTION

Capella (Alpha Aurigae: HR 1708; HD 34029) is a nearby ($d = 13.38$ pc; Barlow, Fekel, & Scarfe 1993) multiple star system in which the brightest components, two G-type giants, form a spectroscopic binary. Capella has been a frequent target for ultraviolet, EUV, and X-ray measurements (Catura, Acton, & Johnson 1975; Dupree 1975; Vitz et al. 1976; Bobroff, Nousek, & Garmire 1984; Ayres 1988; Green et al. 1992). Under the Guest Observer Program for the *EUVE* satellite, we were awarded multiple observations of Capella. The spectral images from the calibration program were made available to us in 1993 April. The spectrometer characteristics are described by Welsh et al. (1990).

2. OBSERVATIONS AND DATA REDUCTION

The spectra were acquired during 1992 December 10–13. Capella was at phase 0.82–0.86 (Barlow et al. 1993, where phase 0.0 corresponds to orbital quadrature with the more massive [cooler] primary star receding with maximum positive velocity). The integration time totaled 68,825 s, 76,128 s, and 75,181 s for the short-wavelength (SW), medium-wavelength (MW), and long-wavelength (LW) spectrometers respectively; the three spectra were obtained simultaneously.

The spectra (Fig. 1) were extracted from summed two-dimensional images by removing an averaged background evaluated on either side of the spectrum. Central wavelengths were determined from Gaussian fits to the spectral lines, and fluxes obtained by summation over the counts in the lines. We removed a small local continuum level from the SW spectrum, assessed by spectral synthesis of the thermal bremsstrahlung contribution. The EGODATA reference set (Vers. 1.7) gave $A_{\rm eff}$ of the spectrometers. The background counts in our SW spectrum decrease from 7.6 near λ90 to 5.0 at λ150. The strong lines represent ≥ 6 σ detections assuming Poisson counting statistics; the weakest line we report (λ145.7) has $S/N \approx 3$.

To correct for interstellar absorption, $N_{\rm H}$ was taken as 1.8×10^{18} cm^{-2} (Linsky et al. 1993); the H/He abundance ratio was set at 11.6 (Kimble et al. 1993), and helium was assumed to be neutral. A software package obtained from the *EUVE* GO Data Bank (Rumph, Bowyer, & Vennes 1993) was modified to compute the interstellar optical depth at each wavelength, and to correct the observed flux listed in Table 1. The *EUVE* detectors suffer from a fixed pattern noise due to small spatial scale periodic distortions (Vallerga et al. 1991), which can cause line flux to be slightly shifted in wavelength but not intensity. We conservatively identify only the strongest spectral features except where members of a multiplet are present.

3. LINE IDENTIFICATIONS

Because knowledge of the relative and absolute wavelength scale is at an early stage, we required only that the wavelength coincidence be comparable to the spectral resolution of the spectrometers, namely 0.5 Å (SW), 1.0 Å (MW), and 2.0 Å (LW) (*EUVE* Documentation 1993). In the EUV many candidate lines may exist within this acceptable wavelength coincidence (cf. Kelly 1987), and additional criteria are required. We look for resonance transitions of abundant elements, predicted line intensity ratios within a multiplet, and consistency with the emission measure distribution. Solar spectra in this region are particularly useful (Doschek & Cowan 1984; Mason et al. 1984; Thomas & Neupert 1993), as are measures of the spectrum from the Princeton Large Torus (PLT) tokamak (Stratton et al. 1985). We use the emission model of Brickhouse, Raymond, & Smith (1993) to predict line fluxes for iron, and earlier codes (Raymond 1988) for other abundant elements. The iron emission model solves the statistical equilibrium equations for a set of fine-structure levels, incorporating the ionization equilibrium of Arnaud & Raymond (1992) and new collision cross sections. The average difference between the observed and identified wavelengths for unblended lines is ± 0.18 Å for the SW (15 lines), ± 0.56 Å for MW (10 lines), and ± 0.23 Å for LW (3 lines).

The Capella spectrum contains several transitions whose relative fluxes are determined by branching ratios. These lines include Fe XVI $\lambda 335.4/\lambda 360.80 = 1.99$ (MW) and 2.15 (LW) as compared to the expected ratio of 2.18 (Fuhr et al. 1981); Fe XVIII, $\lambda 103.94/\lambda 93.92 = 0.39$ as compared to theory (0.38, Mason et al. 1984) and 0.31 from PLT (Stratton et al. 1985); and Fe XIX, $\lambda 111.70/\lambda 101.55 = 0.75$ as compared to 0.76 (PLT) and 0.39 (theory); $\lambda 109.97/\lambda 101.55 = 0.91$ versus 0.51 (theory); $\lambda 120.00/\lambda 108.37 = 0.25$ compared to 0.33 (PLT) and 0.27 (theory). Such agreement provides reassurance that the identifications, extracted fluxes, and calibration are in reasonable order.

[1] Guest Observer, NASA *Extreme Ultraviolet Explorer* (*EUVE*).
[2] Harvard-Smithsonian Center for Astrophysics, 60 Garden Street, Cambridge, MA 02138.
[3] Naval Research Laboratory, Code 4170, Washington, DC 20375.
[4] CASA, University of Colorado, Boulder, CO 80304.

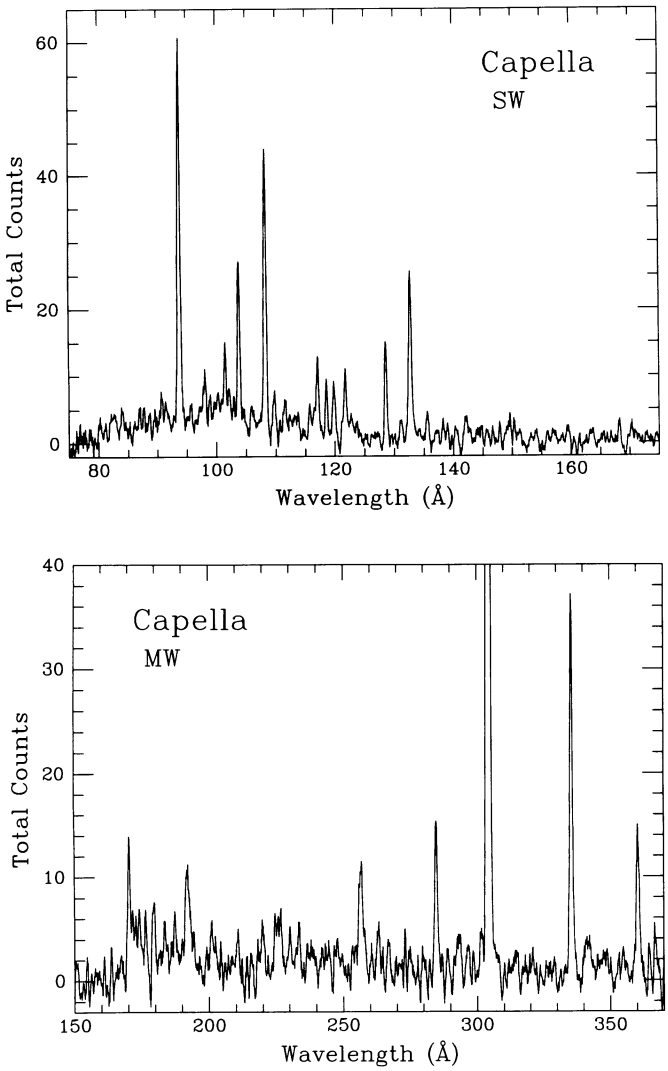

FIG. 1.—The EUV spectrum of Capella as obtained with two spectrometers: SW and MW.

We illustrate line identification procedures with Fe XXIV. Lines from adjacent ions (Fe XXIII and Fe XXII) are present. The emission measure required to produce these species also contributes to Fe XXIV (λ192.02, λ255.09). The doublet member (λ255) is expected to have a flux equal to 0.58 of the λ192 transition (Mason et al. 1984), but it is blended with a strong He II line. Possible blends with Fe XXIV λ192 include the O V triplet (λ192.75, λ192.80, λ192.91) and Ca XVII (λ192.86), predicted to contribute 45% and 25% of the total flux respectively, and Fe XII (λ192.39), which we rule out because other members of the multiplet are not observed. Other lines of O V (λ220.4 and λ248.5) are observed to be within 15% of their predicted values. Thus we conclude that approximately one-third of the λ192 line can be attributed to Fe XXIV.

4. DISCUSSION

The Capella spectrum is dominated by iron lines and shows higher ionization stages than solar active regions. The spectral lines are characteristic of a solar flare, but there is no indication that Capella flared during the observations. The total flux as measured by the LEXAN/B passband (44–240 Å) changed by less than 15% during simultaneous deep pointing measures (Drake 1993).

TABLE 1

STRONG LINES IN EUV CAPELLA SPECTRUM

λ_{obs}(Å)	Ident.	λ_{lab}(Å)	Counts	Flux^{a}_{obs}	$\text{Flux}^{a,b}_{corr}$
Short Wavelength Spectrometer					
91.39	Fe XIX[c]	91.02	34.6	2.58(−4)	2.70(−4)
93.72	Fe XVIII	93.92	474.1	3.43(−3)	3.60(−3)
97.95	Fe XXI	97.88	61.2	4.28(−4)	4.53(−4)
98.90	Ne VIII	98.11	22.6	1.55(−4)	1.65(−4)
101.44	Fe XIX	101.55	86.3	5.86(−4)	6.24(−4)
102.13	Fe XXI[d]	102.35	39.2	2.67(−4)	2.85(−4)
103.76	Fe XVIII	103.94	188.4	1.30(−3)	1.39(−3)
108.20	Fe XIX	108.37	352.7	2.48(−3)	2.67(−3)
109.71	Fe XIX	109.97	73.2	5.29(−4)	5.71(−4)
111.49	Fe XIX	111.70	58.6	4.35(−4)	4.71(−4)
117.03	Fe XXII	117.17	104.0	8.79(−4)	9.63(−4)
118.57	Fe XX	118.66	61.1	5.35(−4)	5.88(−4)
119.83	Fe XIX	120.00	67.8	6.16(−4)	6.79(−4)
121.72	Fe XX	121.83	72.7	7.00(−4)	7.75(−4)
128.53	Fe XXI	128.73	105.1	1.22(−3)	1.37(−3)
132.66	Fe XXIII[e]	132.85	225.5	3.01(−3)	3.41(−3)
135.50	Fe XXII[f]	135.73	33.3	4.84(−4)	5.53(−4)
142.20	Fe XXI	142.16	36.3	6.67(−4)	7.76(−4)
145.72	Fe XXI	145.65	15.5	3.17(−4)	3.73(−4)
Medium Wavelength Spectrometer					
170.28	Fe IX	171.08	128.1	3.37(−3)	4.27(−3)
172.30	O V[g]	172.17	23.5	5.71(−4)	7.30(−4)
174.06	O VI	173.08	62.3	1.54(−3)	1.99(−3)
183.56	O VI	183.94	57.3	1.51(−3)	2.00(−3)
192.09	Fe XXIV[h]	192.02	149.9	4.28(−3)	5.76(−3)
219.97	O V	220.35	57.1	1.97(−3)	3.13(−3)
256.55	He II[i]	256.32	132.95	5.14(−3)	9.96(−3)
284.74	Fe XV	284.15	152.4	5.27(−3)	1.24(−2)
293.09	Ni XVIII	291.97	52.4	1.76(−3)	4.40(−3)
304.34	He II	303.78	2206.7	6.90(−2)	1.88(−1)
335.50	Fe XVI	335.41	337.9	9.86(−3)	3.52(−2)
360.31	Fe XVI	360.80	156.7	3.88(−3)	1.77(−2)
Long Wavelength Spectrometer					
304.02	He II	303.78	2247.7	5.34(−2)	1.45(−1)
335.22	Fe XVI	335.41	480.3	8.63(−3)	3.07(−2)
360.53	Fe XVI	360.80	241.96	4.02(−3)	1.43(−2)
368.21	Mg IX[j]	368.07	81.6	1.37(−3)	6.80(−3)

[a] Units of photons $cm^{-2} s^{-1}$ at Earth.
[b] Corrected for $N_H = 1.8 \times 10^{18}$ cm^{-2}.
[c] Blended with Fe XXI, λ91.28.
[d] Blended with O VIII, λ102.49.
[e] Blended with Fe XX, λ132.85.
[f] Blended with O V, λ135.52.
[g] Blended with O VI, λ172.9, λ173.0.
[h] Blended with O V, λ192.75, λ192.80, λ192.91 and Ca XVII, λ192.86.
[i] Blended with Fe XXIV, λ255.09.
[j] Blended with Fe XIII, λ368.12.

The SW spectrum shows a background continuum, peaking at λ100, that reflects the effective area curve of the SW spectrometer. Our spectral synthesis of this region confirms that the continuum is real and well matched by a combination of thermal bremsstrahlung and a confluence of unresolved emission lines.

4.1. *The* He II *Lines*

The strongest emission line in the Capella spectrum is the resonance transition of He II (λ303.78). The λ304 airglow is spatially and spectrally extended, so it is clear that the measured emission arises from Capella.

We can predict the λ304 flux. Because the lower level of the ultraviolet He II λ1640 line forms the upper level of the λ304

line, a lower limit to the λ304 flux results by assuming that all λ1640 photons cascade to the λ304 line. (Collisional excitation would increase the λ304 flux.) Ayres (1988) reports 0.47 photons cm^{-2} s^{-1} in λ1640 from Capella (Aa + Ab) which implies a λ304 flux 3 times larger than observed. Resonant scattering by interstellar He^+ might reduce the observed λ304 flux. A λ304 line as luminous as predicted from the λ1640 flux would produce an He^+ Strömgren sphere $\frac{2}{3}$ pc in radius in an interstellar medium of density 0.1 cm^{-3}, with a column density log $N_{He^+} = 16.3$ cm^{-2}. While this would produce a saturated absorption line, it seems unlikely to reduce the broad emission line by more than a factor of 2. Another possibility is absorption by neutral material in Capella's atmosphere. A stellar wind, suggested by the asymmetric Lyα profile, broad and shifted O VI (Dupree 1975) or previous nondetections of He II (Bobroff et al. 1984; Green et al. 1992), might absorb the He II line.

The spectrum of Capella can be measured directly to predict the recombination contribution to λ1640 (Hartmann, Dupree, & Raymond 1982). We observe 0.1 photons cm^{-2} s^{-1} in the 80–228 Å band of EUVE, and the TGS observation of Lemen et al. (1989) implies 0.03 photons cm^{-2} s^{-1} between 40 Å and 80 Å. Since 49% of the recombinations of He II yield λ1640 photons at 10^4 K and high density (Hummer 1993), we predict a recombination contribution to the λ1640 intensity of 1.6×10^{-12} ergs cm^{-2} s^{-1}, or about 30% of the value observed by *IUE* (Ayres 1988).

4.2. *The Emission Measure*

The observed line flux determines the emission measure in the system, EM, viz.,

$$\mathrm{EM}\ (T) \equiv \int_{\Delta T} N_e^2\, dV = 4\pi d^2\, \frac{F_{1,2}}{\epsilon_{1,2}}\ (\mathrm{cm}^{-3})\,, \qquad (1)$$

where we assume that all of the radiation emerges from the emitting volume. Here, the observed flux $F_{1,2}$ (photons cm^{-2} s^{-1}) must be corrected for interstellar absorption, d (cm) is the distance to Capella, and $\epsilon_{1,2}$ (photons cm^{+3} s^{-1}) depends on excitation rate, element abundance, and fractional ionization of the ion species. Equation (1) assumes mean values of the rates and ionization over the temperature interval $\Delta T(\mathrm{K}) = 0.3$ dex (cf. Doschek & Cowan 1984). The emission measure has been evaluated in two ways: (1) with an approximation to the shape of the ionization equilibrium curve, and values of $\epsilon_{1,2}$ from Doschek & Cowan (1984; with corrections, see Dupree & Kenyon 1991) and Dupree & Goldberg (1967, for Fe XV and XVI); (2) with an integration over temperature of the radiative rates for all ions with concentrations greater than 10^{-6} (Brickhouse et al. 1993) using an emission measure distribution constructed to reproduce the observed line fluxes within a factor of 2. Both emission measure distributions are expressed in units of $\Delta T(\mathrm{K}) = 0.1$ dex (Fig. 2). For comparison, two other distributions are shown that are typical of analyses with spectra of lower resolution. Ultraviolet lines are included to define the emission measure below 10^6 K. The continuous emission measure distribution ("IFIT" in Fig. 2) predicts continuum emission from thermal bremsstrahlung in good agreement with the observations, implying that the high-temperature emission measure must cut off approximately as shown.

The emission measure determined by the full integration falls below the approximate values derived for each line. This behavior is expected because the approximation ascribes the emission only to a restricted temperature range where the concentration of a particular species is maximized. In contrast, the numerical integration calculates line flux contributions at temperatures away from the peak values, diminishing the amount of material required at the peak temperature to reproduce the observed flux. Also, the two methods use different ionization equilibria and atomic parameters. It is reassuring to see the basic features of the Capella emission measure occur with both methods.

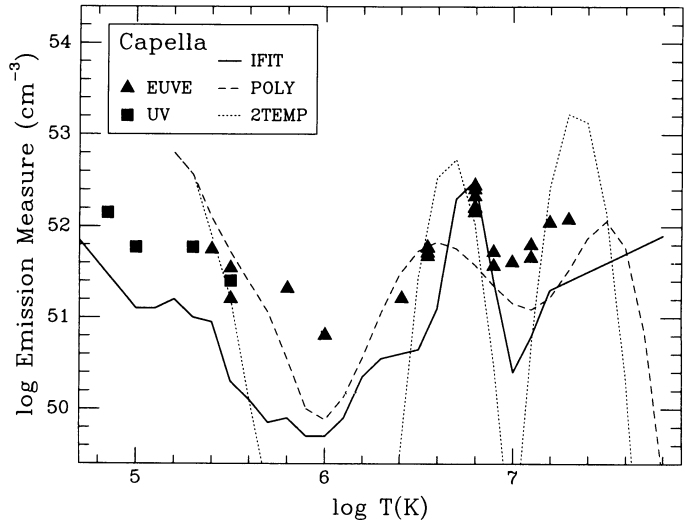

FIG. 2.—The emission measure in the Capella system as defined by the line fluxes (*solid triangles*) from the *EUVE* spectrum. The solid line (IFIT) represents our calculation using a full integration that best represents the observed fluxes. The filled squares denote emission measures determined from *IUE* measures of Si IV, C IV, and N V (Ayres 1988), an O VI observation from *OAO 3* (*Copernicus*; Dupree 1975), and $\epsilon_{1,2}$ values from Jordan et al. (1987) and Dupree & Goldberg (1967). The curves denoted by broken lines (2TEMP and POLY) were adopted with modification (see Dupree & Kenyon 1991) from an analysis of Transmission Grating Spectrometer data from *EXOSAT* by Lemen et al. (1989).

Several important conclusions result from these calculations:

1. A continuous distribution of temperatures (10^5–$10^{7.8}$ K) is present in the Capella system. The slope of this distribution is not inconsistent with that of a magnetic arcade of loops (Antichos & Noci 1986), thermal conduction-dominated loops (Rosner, Tucker, & Vaiana 1978), or a corona heated by microflares (Raymond 1990).

2. A minimum in the emission measure distribution is present near 10^6 K. This differs from the solar atmosphere where a minimum occurs near $10^{5.2}$ K. (A modest minimum may be present near 10^5 K, but the emission measure drops precipitously above 10^5 K reaching the deep minimum at 10^6 K.) Since a temperature of $\sim 10^{5.2}$ K marks the maximum in the radiative loss rate for a collisionally ionized plasma under equilibrium conditions, the lack of material in the Sun at these temperatures seems natural. Possibly the anomalous minimum results from a fast wind in the system creating nonequilibrium ionization (Dupree, Moore, & Shapiro 1978), or several components of emission (one or both giant stars perhaps with little high temperature emission, and any interaction region) sum to create an apparent minimum at 10^6 K.

3. Strong lines of Fe XVIII and Fe XIX demand a local increase in the emission measure near $10^{6.8}$ K. This "bump" may be part of a continuous distribution of plasma or may be ascribed to a separate feature in the system. Comparison with solar flare spectra shows that this peak is not an artifact of the emission model. We can speculate that this feature is associated with a magnetically active region (cf. Ayres 1988; Shcherbakov et al. 1990) or results from a shock interface between the stars where their winds collide (Dupree & Kenyon 1991). Time variability of these various features in our subsequent observations may address this question.

4. An unexpected result of our direct integration technique is that quite a few transition region lines, from ions such as Si V (λ117.8), O IV (λ195.8, λ238.5), and Ne V (λ143.33, λ358.9) are weaker than predicted. The emission measure curve at these temperatures is based on the ultraviolet Si IV, C IV, N V, and O VI lines, and is consistent with EUV lines of other ions such as Mg V, O V, and Ne VIII. One explanation might be severe Lyman-continuum absorption of transition region lines as suggested by solar EUV spectra of active regions (Kanno 1979; Doschek & Feldman 1982). Also, departures from ionization equilibrium associated with a downflow (Raymond & Dupree 1978; Doyle et al. 1985) might shift ions such as O IV and Ne V to lower tempeatures, drastically reducing the ratios of the EUV lines to ultraviolet lines.

4.3. *The Electron Density*

Several line ratios in Fe XXI are useful diagnostics of electron density (see Doschek 1991). The Capella spectra indicate ratios (units of ergs cm^{-2} s^{-1}) of $\lambda142.16/\lambda128.73 = 0.51$, $\lambda145.65/\lambda128.73 = 0.24$, and $\lambda102.35/\lambda128.73 = 0.21$ which imply $\log N_e = 13.2$, 12.8 and 11.6 (cm^{-3}), respectively. The λ102.35 line is the strongest member of a multiplet, including λ91.28 (weak and blended with Fe XIX, λ91.02) and λ97.88, which we observe to be 3.8 times stronger than the branching ratio predicts. The weakness of the λ102.3 line in the Capella spectrum contrasts with its dominance in some solar flares (Mason et al. 1979, 1984) and in the high-density PLT (Stratton et al. 1985).

Thus it appears that the density in Capella is $\approx 4 \times 10^{11}$–10^{13} cm^{-3} at temperatures of $\approx 10^7$ K, implying that the scale of the emitting volume is small $\sim 10^{-3}$ R_*. While the range of density predictions seems large, and we cannot consistently account for the λ102.35 multiplet at this time, we note that Fe XXI derives a large fraction of its emission from the local maximum in the emission measure at $10^{6.8}$ K; in the IFIT model, 75% of the λ128.73 flux is produced below the temperature of maximum concentration. The value of $N_e T \approx 4 \times 10^{18}$–$10^{20}$ cm^{-3} K implies electron pressures exceed those in the solar transition region and lie at and beyond the upper bound of pressures in coronal flares (Dosheck 1991). Magnetic fields of several hundred gauss are required to confine such a plasma.

We are grateful to the EUVE Guest Observer Center at the Center for Extreme Ultraviolet Astronomy at UC Berkeley for assistance. Dan Zucker of CfA is appreciated for help with the data and figures. We have made use of the Simbad database, operated at CDS, Strasbourg, France. This research is supported in part by NASA grant NAG5-2330 to the Smithsonian Institution.

REFERENCES

Antiochos, S. K., & Noci, G. 1986, ApJ, 301, 440
Arnaud, M., & Raymond, J. 1992, ApJ, 398, 394
Ayres, T. R. 1988, ApJ, 331, 467
Barlow, D. J., Fekel, F. C., & Scarfe, C. D. 1993, PASP, 105, 476
Bobroff, N., Nousek, J., & Garmire, G. 1984, ApJ, 277, 678
Brickhouse, N. S., Raymond, J. C., & Smith, B. W. 1993, BAAS, 25, 864
Catura, R. C., Acton, L. W., & Johnson, H. M. 1975, ApJ, 196, L47
Doschek, G. A. 1991, in Extreme Ultraviolet Astronomy, ed. R. F. Malina & S. Bowyer (New York: Pergamon), 94
Doschek, G. A., & Cowan, R. D. 1984, ApJS, 56, 67
Doschek, G. A., & Feldman, U. 1982, ApJ, 254, 371
Doyle, J. G., Raymond, J. C., Noyes, R. W., & Kingston, A. E. 1985, ApJ, 297, 816
Drake, J. 1993, private communication
Dupree, A. K. 1975, ApJ, 200, L27
Dupree, A. K., & Goldberg, L. 1967, Sol. Phys., 1, 229
Dupree, A. K., & Kenyon, S. J. 1991, in Extreme Ultraviolet Astronomy, ed. R. F. Malina & S. Bowyer (New York: Pergamon), 69
Dupree, A. K., Moore, R. T., & Shapiro, P. R. 1978, ApJ, 229, L101
EUVE Guest Observer Documentation. 1993, Version 0.1.
Fuhr, J. R., Martin, G. A., Wiese, W. L., & Younger, S. M. 1981, J. Phys. Chem. Ref. Data, 10, 305
Green, J. C., Wilkinson, E., Ayres, T. R., & Cash, W. C. 1992, ApJ, 397, L99
Hartmann, L. H., Dupree, A. K., & Raymond, J. C. 1982, ApJ, 252, 214
Hummer, D. 1993, private communication
Jordan, C., Ayres, T. R., Brown, A., Linsky, J. L., & Simon, T. 1987, MNRAS, 225, 903
Kanno, M. 1979, PASJ, 31, 115
Kelly, R. L. 1987, J. Phys. Chem. Ref. Data, 16, Suppl. 1
Kimble, R. A., Davidsen, A. F., Long, K. S., & Feldman, P. D. 1993, ApJ, 408, L41
Lemen, J. R., Mewe, R., Schrijver, C. J., & Fludra, A. 1989, ApJ, 341, 474
Linsky, J. L., et al. 1993, ApJ, 402, 694
Mason, H. E., Bhatia, A. K., Kastner, S. O., Neupert, W. M., & Swartz, M. 1984, Sol. Phys., 92, 199
Mason, H. E., Doschek, G. A., Feldman, U., & Bhatia, A. K. 1979, A&A, 73, 74
Raymond, J. C. 1988, in Hot Thin Plasmas in Astrophysics, ed. R. Pallavicini (Dordrecht: Kluwer), 3
———. 1990, ApJ, 365, 387
Raymond, J. C., & Dupree, A. K. 1978, ApJ, 222, 379
Rosner, R., Tucker, W. H., & Vaiana, G. S. 1978, ApJ, 220, 643
Rumph, T. R., Bowyer, S., & Vennes, S. 1993, ApJS, submitted
Shcherbakov, A. G., Tuominen, I., Jetsu, L., Katsova, M. M., & Poutanen, M. 1990, A&A, 235, 205
Stratton, B. C., Moos, H. W., Suckewer, S., Feldman, U., Seely, J. F., & Bhatia, A. K. 1985, Phys. Rev. A, 31, 2534
Thomas, R. J., & Neupert, W. M. 1993, ApJ, submitted
Vallerga, J. V., Siegmund, O. H. W., Vedder, P. W., & Gibson, J. L. 1991, Nucl. Inst. Meth. Phys. Res., A310, 317
Vitz, R. C., Weiser, H., Moos, H. W., Weinstein, A., & Worden, E. S. 1976, ApJ, 205, L35
Welsh, B., Vallerga, J. V., Jelinsky, P. L., Vedder, P. W., Bowyer, S., & Malina, R. F. 1990, Opt. Eng., 29, 752